P1.4 Generation of Visibility Map at the Hong Kong International Airport (HKIA) using LIDAR Data

R.L.M. Chan [(a)], P.W. Chan [(b)] * and A.Y.S. Cheng [(a)]
[(a)] City University of Hong Kong, Hong Kong, China
[(b)] Hong Kong Observatory, Hong Kong, China

1. INTRODUCTION

The Hong Kong Observatory (HKO) operates a Doppler LIDAR at HKIA (location in Figure 1) for windshear alerting services. Apart from radial velocity, the LIDAR also outputs, among others, the backscattered power measurements. Chan (2003) discusses the retrieval of visibility using the backscattered power data in hazy weather based on an empirical relationship between the extinction coefficient at the LIDAR's wavelength (about 2 microns) and that for the visible range. The visibility so determined is found to compare well with the observations from the forward scatter sensors (FD12P, locations in Figure 1) in selected cases of hazy weather at HKIA.

This paper presents the development of a new algorithm that combines the LIDAR's backscattered power and measurements from the forward scatter sensors to generate visibility map in the vicinity of HKIA in different weather situations, without the use of the empirical relationship for a specific weather type. The methodology to generate the map is described in Section 2. The map is found to reveal many interesting features of visibility distribution at HKIA. Some examples are shown in Section 3. The conclusions of this paper are given in Section 4.

2. GENERATION OF VISIBILITY MAP

The LIDAR at HKIA performs the following scans regularly:

(a) Plan-position Indicator (PPI) scans at elevation angles of 0, 1 and 4.5 degrees;
(b) Range-height Indicator (RHI) scans at a couple of azimuth angles; and
(c) Glide-path scans along all the eight glide paths of HKIA.

In the present study, only the backscattered power data obtained in 1-degree PPI scans of the LIDAR are used to retrieve the horizontal variation of visibility in the airport area.

Klett's inversion method (Klett, 1981) is employed to firstly retrieve extinction coefficient $\sigma(r)$ from the LIDAR's backscattered power $P(r)$ along a radial, where r is the range from the LIDAR. Near range correction to the backscattered power due to the optics of the LIDAR (as provided by the LIDAR manufacturer) has been applied before the retrieval. Rayleigh scattering from molecules in the air is not considered in Klett's method, but this is expected to have a negligible contribution for the wavelength of the LIDAR. The extinction coefficient is given by the following equation:

* *Corresponding author address:* P.W. Chan, Hong Kong Observatory, 134A Nathan Road, Hong Kong email: pwchan@hko.gov.hk

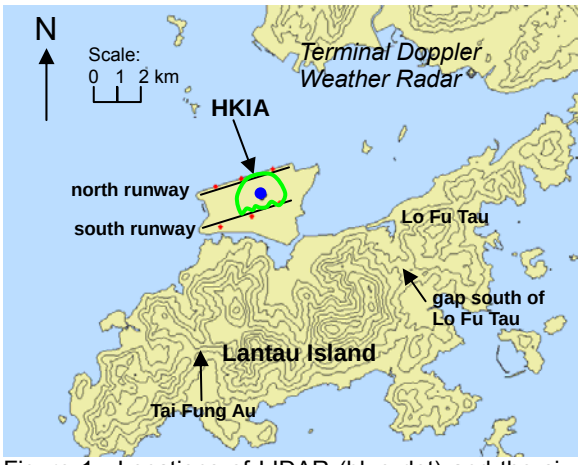

Figure 1 Locations of LIDAR (blue dot) and the six forward scatter sensors (red dots) inside HKIA. The near range "circle" (Section 2) is shown in light green. Height contours are in 100 m.

$$\sigma(r) = \frac{\exp[(S(r) - S_m)/k]}{\left\{\sigma_m^{-1} + \frac{2}{k}\int_r^{r_m}\exp[(S(r') - S_m)/k]dr'\right\}} \qquad (1)$$

for r less than a reference distance r_m, where $S(r) = \ln(r^2P(r))$ is the logarithmic range-adjusted power, $S_m = S(r_m)$, $\sigma_m = \sigma(r_m)$ and k a constant depending on the LIDAR wavelength and the properties of the aerosol. In Klett's method, the aerosol backscatter coefficient β is assumed to be related to the extinction coefficient of the air σ by a power law $\beta \propto \sigma^k$. As in Chan (2003), k is assumed to be 1 in this paper.

The reference distance r_m is taken as the farthest range from the LIDAR with a sufficiently large signal to noise ratio (> -5 dB) or the range at which the LIDAR meets a stationary hard target (such as building and terrain), whichever is shorter. However, the extinction coefficient at the reference distance is in general not available. In our method, it is estimated by using the harmonic mean of the visibility measurements from the six forward scatter sensors within HKIA. σ_m is then obtained from this average visibility value using the following relationship between visibility V at the middle of the visible range (0.55 micron) and σ (Hinkley, 1976):

$$V = \frac{3.91}{\sigma}\left(\frac{0.55}{\lambda}\right)^{1.3} \qquad (2)$$

where λ is the wavelength of the LIDAR.

After the Klett's inversion, an adjustment is made to the whole extinction coefficient profile (as a function of range) based on the measurements from the forward scatter sensors. First of all, the extinction coefficient at the near range location σ_n is read out from this extinction coefficient profile. The near range location is taken as the point of

intersection between the radial and a near range "circle" with a radius of approximately 1 km (location in Figure 1). A reference extinction σ_r is then determined at this near range location. It is calculated by a weighted average of the extinction coefficient values from the six forward scatter sensors following the relationship in Eq. (2). The radial basis function (Hon and Schaback, 2001) is employed to compute the weighted average:

$$\sigma_r = \frac{\sum_{i=1}^{6} w_i \sigma_i}{\sum_{i=1}^{6} w_i} \quad \text{with} \quad w_i = 1/d_i^2 \qquad (3)$$

where d_i is the distance between sensor i and the near range location and σ_i the extinction coefficient from the sensor. The difference between σ_n and σ_r is used to offset the whole extinction coefficient profile. The process is repeated for every measurement radial of the LIDAR.

The visibility map is generated from the extinction coefficient distribution using Eq. (2). For the maps presented in this paper, the visibility data have been smoothed by a moving average both azimuthally (9 to 11 degrees) and radially (three range gates, i.e. about 300 m).

3. EXAMPLES OF VISIBILITY DISTRIBUTION

Three examples of visibility map in different weather conditions are discussed below.

3.1 1 April 2004 – bands of mist

The visibility was good inside HKIA in the early morning on that day, ranging between 9 and 11 km as measured by the forward scatter sensors. However, the visibility map (Figure 2a) shows that there was a band of relatively low visibility of about 4 km stretching from the gap south of Lo Fu Tau (location in Figure 1) to the north of HKIA. As depicted in the LIDAR's velocity image (Figure 2b), east to southeasterly wind prevailed in this low visibility band.

Mist was reported in the area upstream of Lantau Island at that time, with the visibility falling to about 3000 m at the HKO headquarters. From the radiosonde measurement at 8 a.m. on that day (HKT = UTC + 8 hours), there was an inversion of several degrees between 280 and 450 m (Figure 2c). The stable temperature profile near the ground favoured the blockage of the prevailing easterly flow by the high mountains of Lantau Island (with peaks rising to about 1 km AMSL). On the other hand, the easterly wind managed to climb over the lower valleys, such as the gap to the south of Lo Fu Lau (about 150 m AMSL) and brought along the mist from the upstream area. As a result, a curving band of mist appeared to the east and north of HKIA. Another band of low visibility over the western part of HKIA (Figure 2a) may be related to the flow emerging from Tai Fung Au (location in Figure 1).

3.2 20 May 2004 – localized clearance of mist

A late season surge of northerly wind affected the south China coast in the early morning on that day. It was misty with light rain over HKIA shortly after midnight, with the visibility falling to as low as 1800 m. Northwesterly wind picked up slightly afterwards and the dew point at HKIA fell by 1 degree between 2 and 3 a.m. The visibility became higher inside and to the north of HKIA, increasing to about 5 – 6 km (Figure 3a). At the same time, relatively low visibility of 2 – 3 km persisted to the east and west of the airport. In contrast, the LIDAR velocity image (Figure 3c) depicted a rather uniform northwesterly flow in the whole airport area.

The weak plunge of slightly drier air (as revealed in the drop of dew point) cleared up the mist in the vicinity of HKIA. The visibility increased to 6 km or above later in the morning (Figure 3b).

3.3 8 January 2005 – haze in northwesterly wind

Visibility was about 6 km and weak easterly wind prevailed at the airport area in the evening of that day. Northwesterly wind spread southwards over the Pearl River Estuary and reached the northern part of HKIA at about 10:30 p.m. Visibility deteriorated over the north runway, falling below 5 km in haze as measured by the forward scatter sensors. On the other hand, the south runway was mainly affected by the prevailing easterly wind and the visibility was around 6 km over there. The visibility map (Figure 4a) also showed that the haze was not uniform. The visibility was much higher (reaching about 8 km) at a couple of kilometres to the north of HKIA. At the same time, it was as low as 2000 m just to the northeast of the airport where northwesterly wind converged with the prevailing easterly (Figure 4b).

4. CONCLUSIONS

This paper describes an algorithm to generate visibility map using the backscattered power data from a Doppler LIDAR and the visibility measurements from a limited number of forward scatter sensors within the coverage of the LIDAR. Klett's inversion method is employed but with the following modifications: (i) the extinction coefficient at the reference range is estimated from the harmonic average visibility value from the forward scatter sensors as a first guess, and (ii) the retrieved extinction coefficient profile is offset by comparing with a distance-dependent, weighted average of the visibility readings from the forward scatter sensors.

The visibility maps so obtained are found to reveal many interesting features of the variation of visibility in the vicinity of HKIA. They could be applied to different kinds of low visibility weather, such as mist and haze. Compared to in situ visibility measurements, for instance, from forward scatter sensors, the LIDAR-based visibility maps greatly extend the monitoring area and would be useful in the short-term forecasting of low visibility conditions for aviation and other applications. Of course, due to rapid attenuation of the laser beam in very humid air, the visibility map will have limited application value in fog and heavy rain.

Acknowledgement

The author (PWC) would like to thank the LIDAR

manufacturer, Lockheed Martin Coherent Technologies, for providing the technical information required for near-range correction of the backscattered power data.

References

Chan, P.W., 2003: Application of LIDAR backscattered power to visibility monitoring at the Hong Kong International Airport: some initial results. *6th International Symposium on Tropospheric Profiling: Needs and Technologies*, Leipzig, Germany.

Hinkley, E., 1976: *Laser Monitoring of the Atmosphere*. Springer-Verlag, 416 pp.

Hon, Y.C., and R. Schaback, 2001: On unsymmetric collocation by radial basis functions, *Applied Mathematics and Computation*, **119**, 177-186.

Klett, J.D., 1981: Stable analytical inversion solution for processing lidar returns, *Applied Optics*, **20**, 211-220.

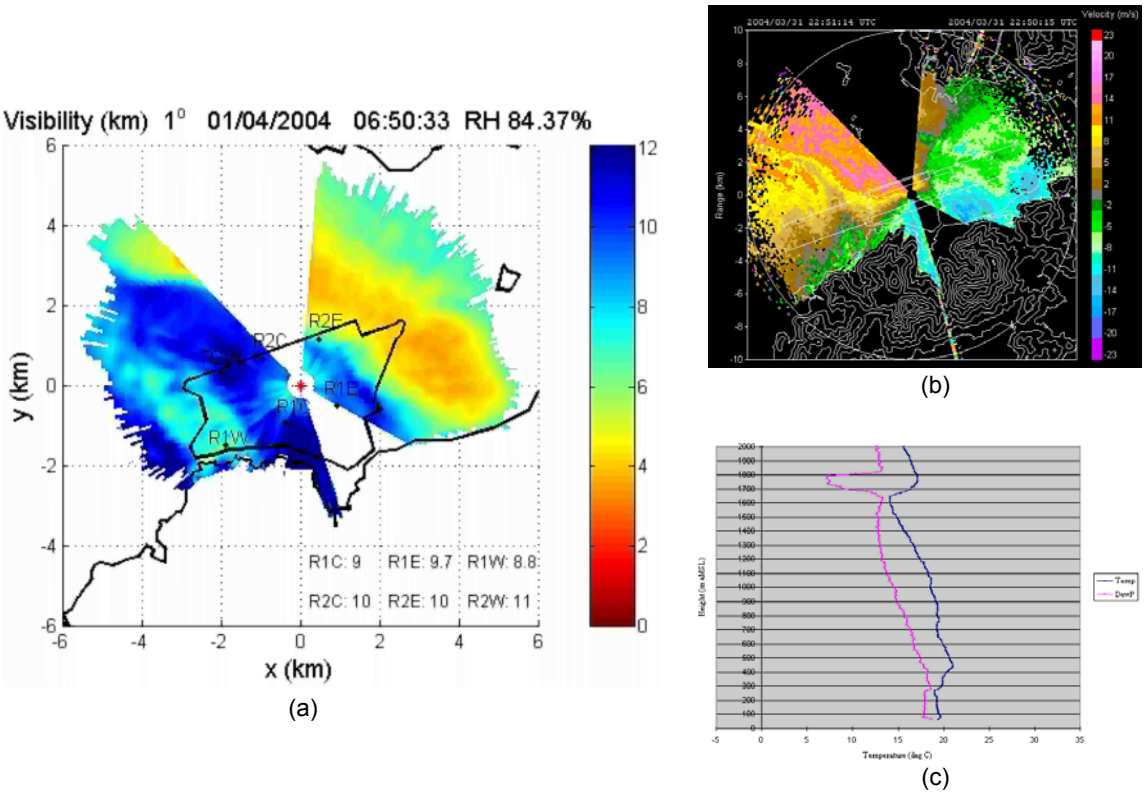

Figure 2 The LIDAR-based visibility map at 6:51 a.m., 1 April 2004 (a). The colour scale of visibility is in km. The forward scatter sensor readings are shown in the lower right of the figure, whereas the relative humidity measured at HKIA is given at the top. (b) is the LIDAR's radial velocity image in 1-degree PPI scan at the same time. The colour scale of velocity is in m/s. Warm/cool colour refers to the wind blowing away/towards the LIDAR. (c) shows the temperature (blue) and dew point (pink) profiles up to 2000 m AMSL as measured by the radiosonde in Hong Kong at 8 a.m., 1 April 2004.

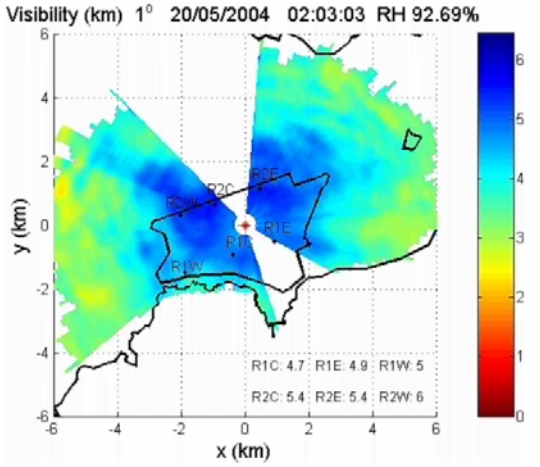

(a)

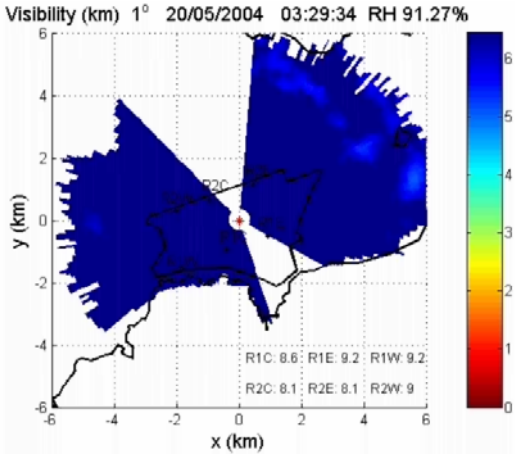

(b)

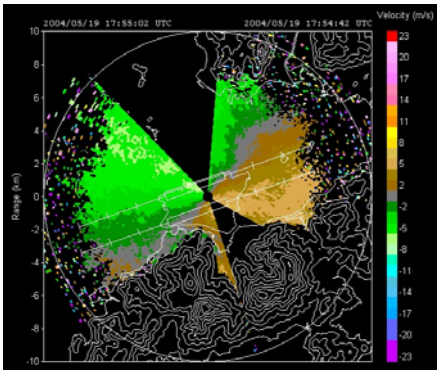

(c)

Figure 3 (a) and (b) are the LIDAR's visibility maps at about 2 a.m. and 3:30 a.m. respectively on 20 May 2004. (c) is the velocity image at about the same time as in (a).

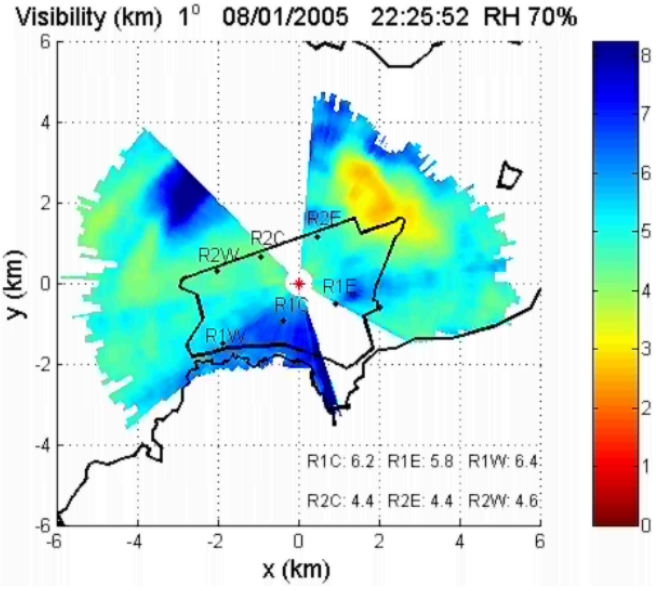

(a)

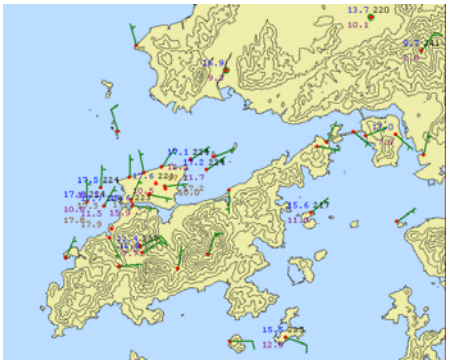

(b)

Figure 4 (a) is the LIDAR visibility map at 10:26 p.m., 8 January 2005. The wind measurements of the automatic weather stations (red dots) around HKIA at that time are shown in (b) as green wind barbs.